

---

This is the **accepted version** of the journal article:

Herraiz-Martínez, Francisco Javier; Paredes, Ferran; Zamora González, Gerard; [et al.]. «Printed Magnetoinductive-Wave (MIW) delay lines for chipless RFID Applications». IEEE transactions on antennas and propagation, Vol. 60, issue 11 (Nov. 2012), p. 5075-5082. DOI 10.1109/TAP.2012.2207681

---

This version is available at <https://ddd.uab.cat/record/288474>

under the terms of the  <sup>IN</sup>  
COPYRIGHT license

# Printed Magnetoinductive-Wave (MIW) Delay Lines for Chipless RFID Applications

Francisco Javier Herraiz-Martínez, *Member, IEEE*, Ferran Paredes, Gerard Zamora, Ferran Martín, *Fellow, IEEE*, and Jordi Bonache, *Member, IEEE*

**Abstract**—A novel fully passive and electromagnetic chipless radiofrequency identification (RFID) system is proposed. The system is based on printed tags implemented with magnetoinductive-wave (MIW) delay lines. Such lines are composed of a periodic array of coupled square split ring resonators (SSRRs) and propagate slow waves. The tag is codified by introducing reflectors (which provide the identification signature) between the elements of the array. When the tags are interrogated with a pulse in time domain, they produce replicas at the positions where the reflectors are placed. Thanks to the slow group velocity of the MIW delay line, the replicas of the original pulse are not overlapped in time domain and can be demodulated, thus providing the identification code of the tag. The design considerations to implement these chipless tags are studied in the present work. Moreover, a complete set of codified MIW lines for a two-bit system is designed, manufactured and measured. The reported experimental results validate the proposed approach.

**Index Terms**—Chipless tags, magnetoinductive waves (MIWs), passive tags, radio frequency identification (RFID).

## I. INTRODUCTION

RADIO frequency identification (RFID) is the contactless and automatic technology based on electromagnetic waves used to identify people and objects [1]. A typical RFID system consists of two types of elements: the reader and the tags. A tag with a different identification code is attached to any object to be recognized by the system. By continuously sending identification queries, the reader interrogates those tags located within the read range, and the tags reply to the reader with their identification codes.

Most tags consist of two elements: an antenna and an application specific integrated circuit (ASIC) chip [2]–[3]. Although tag cost has been considerably decreased in recent years, further reduction is crucial for some applications such

as tagging low-cost items. Since the bottleneck to achieve cheaper tags is the presence of the chip, the development of low-cost chipless tags is of paramount importance [4]. If such tags were cost competitive and exhibited reasonable performance, they may replace the optical barcodes. Thus, the development of chipless RFID tags is the keystone for the implementation of “RF barcodes” [4].

Several chipless RFID systems have been reported in the literature [4]. The first ones, reported in the seventies, are based on piezoelectric delay lines which propagate surface acoustic waves (SAWs) [5]. These tags are composed of an antenna, a SAW delay line, and an electro-acoustic transducer. The operation of the system is as follows: the reader transmits a pulse via an electromagnetic signal which is received by the tag antenna. The antenna transfers the pulse to the SAW delay line through the transducer. Then, the pulse is propagated through the SAW delay line which contains reflectors. These reflectors generate replicas of the original pulse in the time domain. Thus, the identification signature of each tag is codified by the presence or absence of reflectors in the delay line. Finally the replicas produced by the SAW delay line are transmitted to the reader which detects the tag identification code. This technology has been used for decades for remote sensing and identification [6]. One of the main advantages of these systems is that they are narrowband. Therefore, they can be designed for one of the regulated RFID bands. In particular, a global SAW tag technology in the ISM band of 2.45 GHz was proposed in 2002, and is being commercialized [7]. However, the SAW tags are composed of two different elements as they combine piezoelectric materials and an antenna, and this could increase the price of the tags. Hence, these SAW-based tags do not seem a good solution for replacing optical barcodes.

A fully electromagnetic approach might be a possible solution to circumvent the high cost of SAW technology. In that case, low-cost inks and substrates, such as paper, could be used. There are some proposals of fully electromagnetic chipless tags [8]–[13] in the literature. Most of these proposals are based on codifying the identification signature in the spectrum of the response signal. These tags are implemented by using resonators with different resonance frequencies. When the tag is interrogated with a broadband signal, its response presents spectral components (the identification code) at the resonance frequencies of the tag resonators. The main drawback of this frequency-domain approach is the

Manuscript received December 6, 2011. This work was supported by the Spanish MICINN (projects CSD2008-00066, TEC2010-17512 and EXPLORA TEC2011-13893-E), and by AGAUR (Generalitat de Catalunya) through project 2009SGR-421.

F. J. Herraiz-Martínez was with GEMMA/CIMITEC, Departament d'Enginyeria Electrònica, Universitat Autònoma de Barcelona, Bellaterra (Barcelona), 08193, Spain. He is now with Department of Signal Theory and Communications, Carlos III University in Madrid, Leganés (Madrid), 28911, Spain. (e-mail: fjherraiz@tsc.uc3m.es).

F. Paredes, G. Zamora, F. Martín and J. Bonache are with GEMMA/CIMITEC, Departament d'Enginyeria Electrònica, Universitat Autònoma de Barcelona, Bellaterra (Barcelona), 08193, Spain.

intrinsic broadband nature of the spectral signature, which is contrary to RFID regulations [1].

Recently, artificial left-handed (LH) delay lines have been proposed as an alternative to SAW delay lines for chipless RFID applications [14]-[15]. LH lines exhibit low group velocities as compared to conventional transmission lines. However, group velocities significantly below  $c/10$ , where  $c$  is the speed of light in vacuum, are difficult to obtain, and this seems insufficient for practical applications. Specifically, bandwidths around 20% have been needed to detect the response of the tags in practical situations using this approach. Moreover, these LH delay lines have been implemented by soldering lumped components to conventional transmission lines, which increases the tag cost.

In this paper, a novel chipless RFID system is proposed. The tags are composed of an antenna and a planar magnetoinductive-wave (MIW) delay line. Both elements are fully printable on one side of a dielectric substrate. The MIW delay line supports magnetoinductive waves, i.e., slow waves propagating along magnetically coupled resonators [16]. These slow wave structures exhibit group velocities as small as  $c/100$ , and this allows RFID operation by using only a narrow band of the electromagnetic spectrum. Moreover, tag dimensions can be confined within reasonable limits as well. In this paper, the ISM band of 2.45 GHz is used in order to provide a global solution. The paper is mainly focused on the design of the codified MIW delay lines for the proposed system.

The outline of this paper is as follows. The general system architecture is presented in Section II. Then, the basic theory of planar MIWs is reviewed in Section III. The next Section is focused on the design of the delay lines based on MIWs and the study of the trade-offs needed to implement the chipless tags. The design and measurement of a set of two-bit MIW delay lines complete this Section. The paper ends with a discussion on the advantages and limitations of chipless tags (Section V) and with the main conclusions (Section VI).

## II. GENERAL DESCRIPTION OF THE CHIPLESS RFID SYSTEM

The conceptual sketch of the proposed system is shown in Fig. 1. The two typical elements of a RFID system, the reader and the tag, are present, but in this case the tag is chipless. The proposed tags are completely planar and printed on a grounded dielectric substrate. The tags are composed of a printed antenna, one or several microstrip lines, and a chain of squared split ring resonators (SSRRs). The printed antenna is used to communicate with the reader. The chain of SSRRs acts as a delay line which allows the propagation of MIWs. A microstrip line connected to the antenna and inductively coupled to the first SSRR of the array, serves as the transducer between the microstrip mode and the MIW, as it was demonstrated in [17]. Finally, the additional microstrip lines are coupled between specific pairs of SSRRs and are used to implement the digital identification code of the tag. Thus, the location of these lines is different for each tag.

The chipless RFID system operates in the following way. The reader sends a modulated pulse with a carrier at  $f_0$ . This

pulse is received by the printed antenna of each tag within the read range of the system. Then, for each tag, the pulse is transmitted to the SSRRs array through the microstrip line. Partial reflections of the pulse are generated at the positions where the coupled microstrip lines are placed. These partial reflections of the original pulse are sent back to the reader through the antenna. These replicas of the original pulse are detected by the reader which identifies the tag. The key point of the system is the use of the delay lines in the tags, which allows the propagation of MIWs with slow group velocities. This avoids the overlapping of pulse replicas in time domain so that they can be detected by the reader. For this reason, this paper is focused on the design considerations of the MIW delay lines without taking into account the wireless link, which will be studied in future works.

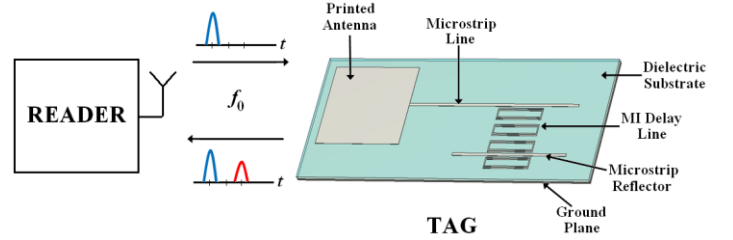


Fig. 1. Sketch of the proposed chipless RFID system.

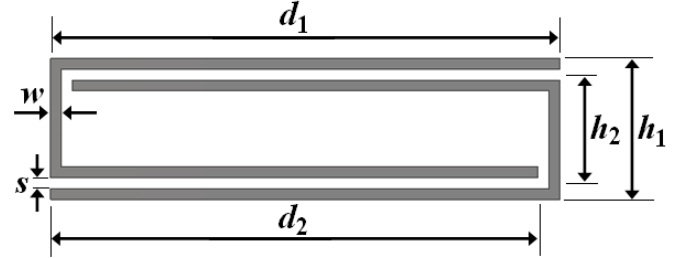


Fig. 2. Geometry of the SSRR particle used as the periodic element of the MI delay line.

## III. MIWS IN PLANAR TECHNOLOGY

MIWs are slow waves which can propagate along periodic structures where the elements are magnetically coupled [16]. The first MIW waveguide was a one-dimensional array of capacitively loaded metallic loops arranged along the axis of a dielectric rod [19]. After that, MIW were also reported in one, two and three dimensions supported by different types of resonators [19]-[21]. The transduction of MIWs in planar technology was proposed in [17]. This was done with a pair of 50- $\Omega$  microstrip lines coupled to an array of magnetically coupled resonant elements. The distance between the open end of the microstrip line and the axis of the array is a quarter wavelength at the resonance frequency of the elements, in order to maximize the coupling between the microstrip lines and the array. The same approach is used in the present work. The resonant element is the SSRR, which is a square version of the well-known split ring resonator (SRR) [16], as it is shown in Fig. 2. This geometrical variation is introduced in order to enhance the coupling between adjacent elements of the array. The equivalent circuit model of a SSRR is a LC

parallel tank [22], which allows computing the resonant frequency as

$$\omega_0 = \sqrt{\frac{2}{d_2 LC_{\text{pul}}}} \quad (1)$$

where  $d_2$  is the overlapped length between the two long arms of the SSRR,  $L$  is the total inductance of the SSRR and  $C_{\text{pul}}$  is the per unit length capacitance between the long arms. The values of  $L$  and  $C_{\text{pul}}$  can be computed from the formulas of a pair of coupled strips [23]. In particular, the value of  $L$  can be obtained by considering a pair of coupled strips with separation  $h_2$ , width  $w$  and length  $d_1$ . In the same way,  $C_{\text{pul}}$  is obtained from a pair of coupled strips with separation  $s$  and width  $w$ .

The dispersion relation of the MIWs in planar configuration without considering losses can be written as [17]

$$\frac{\omega_0^2}{\omega^2} = 1 + 2 \frac{M}{L} \cos(\beta a) \quad (2)$$

where  $\omega$  is the angular frequency,  $\beta$  is the propagation constant,  $a$  is the period of the SSRR chain (or the centre-to-centre separation between SSRRs), and  $M$  is the mutual inductance between adjacent elements.  $M$  can be computed from the coupling between a pair of SSRRs separated a distance  $a$ . Each SSRR is modelled as a pair of wires with opposite currents separated at a distance  $h_2$  and with length  $d_1$  and width  $w$ . The mutual inductance,  $M$ , takes negative values, and wave propagation is backward in this configuration [17]. Thus, the dispersion relation (2) can be rewritten as

$$\beta = \frac{-1}{a} \cos^{-1} \left\{ \frac{L}{2M} \left( \frac{\omega_0^2}{\omega^2} - 1 \right) \right\} \quad (3)$$

where the negative sign is considered to guarantee the backward wave nature in the line.

MIW propagation is allowed in those regions where the propagation constant, given by (3), is real, namely:

$$\frac{\omega_0}{\sqrt{1 - \frac{2M}{L}}} \leq \omega \leq \frac{\omega_0}{\sqrt{1 + \frac{2M}{L}}} \quad (4)$$

Finally, the group velocity of the line,  $v_g$ , is obtained as

$$v_g = \left( \frac{\partial \beta}{\partial \omega} \right)^{-1} = a \frac{-M}{L} \frac{\omega^3}{\omega_0^2} \sqrt{1 - \left[ \frac{L}{2M} \left( \frac{\omega_0^2}{\omega^2} - 1 \right) \right]^2} \quad (5)$$

Considering the previous expressions, it is clear that the MIW delay lines exhibit a dispersive behavior. This could be a limiting factor because the presence of dispersion implies the broadening of signals in time domain. However, since dispersion is unavoidable, the MIW lines are designed in such a way that the pulses in time domain are separated and the identification code of each tag can be demodulated, as it will be shown in the next Section.

#### IV. TWO-BIT CHIPLESS TAGS

##### A. Design Considerations of the MIW Delay Lines for Chipless Tags Application

In order to design the delay lines for the chipless tags, it is necessary to compute the relation between the number of bits that can be stored and the physical parameters of the lines. The number of bits that can be stored in a delay line is

$$n_b = \left\lfloor \frac{\Delta \tau}{\tau} \right\rfloor \quad (6)$$

where  $\Delta \tau$  is the total delay of the line working in reflection and  $\tau$  is the temporal width of the pulse sent by the reader. The pulse width depends on the bandwidth of the system. In order to compute the total delay introduced by the MIW lines, the group velocity can be approximated by its value at the central operation frequency of the system,  $\omega_0$ . Thus, the total delay is obtained as

$$\Delta \tau = 2 \frac{n_{\text{SSRR}} a}{v_g|_{\omega_0}} = 2 \frac{L}{-M} \frac{n_{\text{SSRR}}}{\omega_0} \quad (7)$$

where  $n_{\text{SSRR}}$  is the total number of SSRRs which constitute the delay line. The factor 2 is due to the fact that the pulses are sent back to the reader after reflecting. Finally, expression (7) can be introduced in (6) in order to compute the number of bits of a delay line based on SSRRs:

$$n_b = \left\lfloor 2 \frac{L}{-M} \frac{n_{\text{SSRR}}}{\omega_0} \frac{1}{\tau} \right\rfloor \quad (8)$$

As expected, the number of bits of the delay line increases with the number of SSRRs. However, it is desirable to use the smallest possible number of SSRRs, for a certain number of bits, in order to minimize tag dimensions. The central operation frequency and bandwidth are fixed by design or regulatory constraints. This implies that  $\tau$  cannot be chosen. The central frequency is fixed by the inductance,  $L$ , and the per unit length capacitance,  $C_{\text{pul}}$ , according to (1). Usually, the per unit length capacitance is limited by fabrication restrictions, and the inductance is the only degree of freedom to adjust the central operation frequency,  $f_0$ . Thus, the inductance of the SSRRs is fixed once these elements are designed to resonate at the central operation frequency. Hence, the only variable that can be modified in order to increment the number of bits is the mutual inductance between the SSRRs. This variable can be controlled by the separation between adjacent resonators. If this separation increases, the mutual inductance is reduced and, thus, the number of bits also increases. However, the distance between adjacent SSRRs is limited by three main reasons. First of all, the length of the delay line increases with the inter-SSRR distance, which is contrary to tag miniaturization. The second reason is that if the separation between SSRRs increases, the MIW bandwidth is reduced, as is derived from (4). The final one is due to propagation losses, which increase with the distance between adjacent resonators since they are intimately related to the coupling between resonators. In conclusion, a trade-off between the number of bits, line length, bandwidth and losses,

by choosing the appropriate line period,  $a$ , is necessary.

TABLE I  
DEPENDENCY OF THE MIW DELAY LINE CHARACTERISTICS ON THE  
SEPARATION BETWEEN ADJACENT SSRRs

Separation ( $a$ )	Group Delay (transmission)	Losses	Relative Bandwidth
3.50 mm	11 ns	4 dB	7.33 %
3.75 mm	16 ns	5.6 dB	5.13 %
4.00 mm	21 ns	8 dB	3.70 %

The designed MIW lines of this work operate in the 2.4-2.5 GHz ISM band. This band has been chosen because it is unlicensed worldwide and it is used for RFID systems [1]. Moreover, since the same band can be used worldwide, global chipless tags can be developed. This is an important advantage over UHF RFID systems, which have different frequency regulations in each world region [1]. Hence, the central frequency of the system is set to  $f_0 = 2.45$  GHz and the bandwidth allowed in the spectrum for that band is 4.08%. The dimensions of the SSRRs, optimized to obtain this resonance frequency, are  $d_1 = 9.6$  mm,  $h_1 = 2.6$  mm,  $s = w = 0.20$  mm. The substrate is *Rogers RO3010* with dielectric constant  $\epsilon_r = 10.2$  and thickness  $h = 635$   $\mu$ m).

Different simulations have been carried out in *Agilent ADS Momentum* in order to obtain the optimum separation,  $a$ , for the proposed band. In this paper three cases are shown. In all of them, six SSRRs have been used to implement the MIW delay line. Two microstrip lines, acting as transducers, have been coupled to the external SSRRs, as explained in Section III. The results of these simulations are summarized in Table I. The shortest separation (3.5 mm) gives the smallest losses (4 dB) and the widest bandwidth (7.33 %). However, this separation produces the shortest delay (11 ns) which reduces the number of bits that can be stored in the line according to (6). The longest delay (21 ns) is obtained for the largest separation (4 mm). However, this separation implies high losses (8 dB) and a narrow bandwidth (3.70 %), which is not wide enough for the proposed band. These results are consistent with the explanation given before. Thus, the intermediate separation (3.75 mm) implies a trade-off between the delay (16 ns), the losses (5.6 dB), the bandwidth (5.13%) and the total length of the line. For this reason, the separation is finally set to this value.

A prototype MIW delay line has been fabricated and characterized with the aim to experimentally validate the simulated bandwidth and group delay introduced by the line. The simulated and measured S-parameters of the line are plotted in Fig. 3. The insertion losses are 3 dB higher in the experimental results, approximately. This will reduce the incident power in each reflector. Moreover, the matching is somehow worse in the fabricated circuit compared to simulation. Fig. 4 shows the simulated and measured group delay between the two microstrip ports. The passband of the fabricated MIW line extends from 2.32 GHz up to 2.45 GHz. Therefore, the central operation frequency has been shifted down to 2.39 GHz. This slight deviation is mainly due to tolerances in the fabrication process. Nevertheless, the

measured delay at the central operation frequency is 15.5 ns, which is in good agreement with the simulated value.

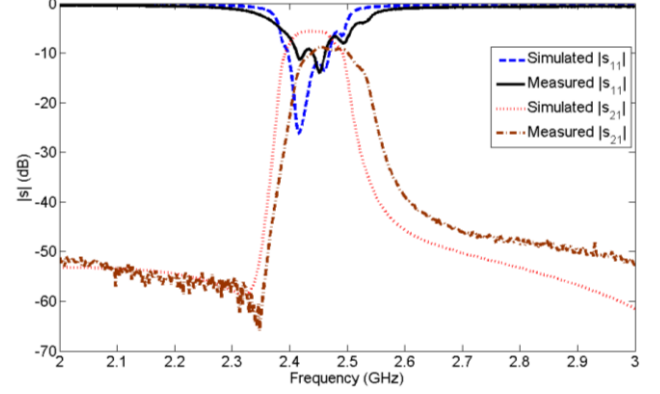


Fig. 3. Simulated and measured S-parameters of the designed MIW delay line.

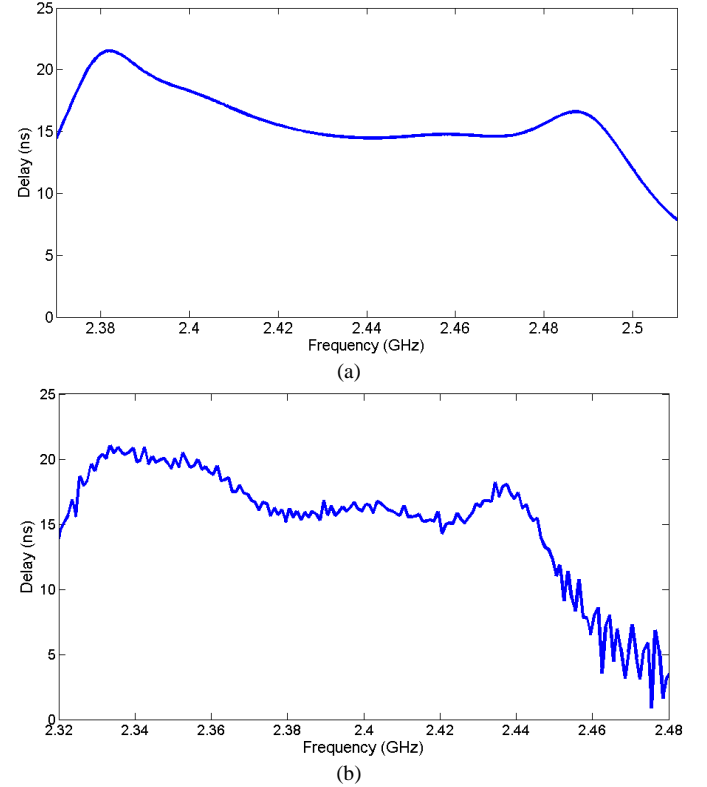


Fig. 4. Group delay between the two microstrip ports of the fabricated MIW line. (a) Simulation results. (b) Experimental results.

Once the group delay has been obtained, the number of allowed bits in the considered delay line can be computed. To this end, it is necessary to determine the temporal width of the pulses. Gaussian pulses are proposed to implement the chipless RFID system. This type of pulse shaping is used in several wireless communication systems such as GSM and Bluetooth. This type of transfer function has a smooth temporal behavior which depends on the  $-3$  dB bandwidth of the baseband signal [24]. In particular, the impulse response of a Gaussian pulse shaping filter is given by

$$h_G(t) = \frac{\sqrt{\pi}}{\alpha} \exp\left(-\frac{\pi^2}{\alpha^2} t^2\right) \quad (9)$$

where the parameter  $\alpha$  is related to the baseband  $-3$  dB bandwidth,  $B$ , through the expression

$$\alpha = \frac{\sqrt{\ln 2}}{\sqrt{2}B} \quad (10)$$

Since the 2.45-GHz IMS band has 100 MHz bandwidth, the bandwidth of the baseband signal must be the half that value, resulting in  $B = 50$  MHz. Thus, as it follows from (10),  $\alpha = 11.8$  ns. Finally, it is necessary to consider a criterion to compute the temporal width of the pulses, as the Gaussian profile has an infinite length in time. In this work, the limit has been considered when the pulse is below 2 % of its maximum. This implies low overlapping between adjacent pulses. Using this criterion,  $\tau = 15$  ns from (9). Considering these values and the measured delay, the number of bits of the line is  $n_b = 2$ , as results from (6). This means that four different identification codes can be implemented with the six-SSRR line. The complete set of two-bit chipless tags based on the proposed MIW delay line is presented in the next Subsection.

### B. Implementation and Experimental Results

In order to design the chipless tags, it is important to define an approach to avoid unwanted reflections at the end of the line and a mechanism to obtain the required reflections at intermediate positions. Since the MIW delay lines are operated in reflection, only the microstrip line coupled to the first SSRR acts as a port. To avoid reflections at the end of the MIW line, which is necessary when the second bit is 0, a microstrip line ended with a matched load is coupled at the end of the MIW delay line. Regarding the second design consideration, the proposed approach to produce reflections consists on using open-ended 50- $\Omega$  microstrip lines placed between the SSRRs. For the case of the two-bit tags, the first bit reflector is placed in the middle of the MIW delay line (between the third and fourth SSRRs in this implementation) and the second bit reflector is placed at the end of the line. When a total reflection is needed, the line acting as reflector must have a length of  $\lambda/2$  at  $f_0$ . This is the situation when no more partial reflections are used (for instance, at the end of the line). In this case, the  $\lambda/2$  lines provide a  $\Gamma = -1$  reflection coefficient in the delay line, since the distance between the open ends and the centre of the line is  $\lambda/4$ . If only a partial reflection is needed, the length of the reflector is made smaller, and only part of the signal is reflected back to the source. The transmitted signal may thus impinge on the additional reflectors if they are present.

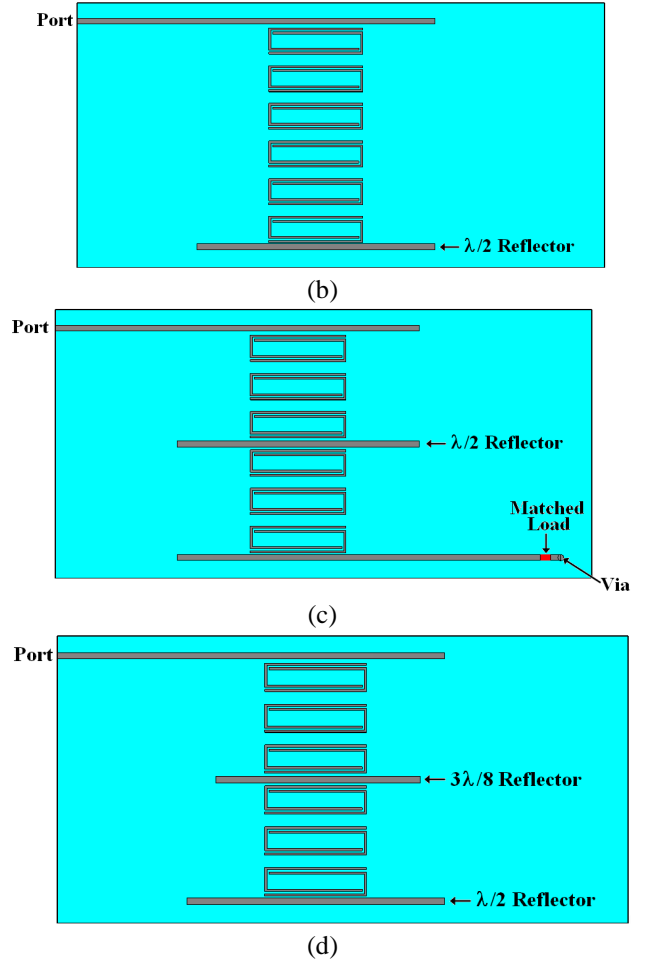
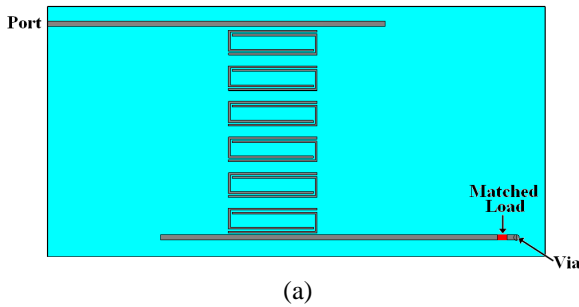


Fig. 5. Layouts of the two-bit chipless tag. (a) 00; (b) 01; (c) 10; (d) 11.

Following the previous design criteria, the final layouts of the four two-bit chipless tag MIW lines are shown in Fig. 5. The tag codified as '00' is similar to the MIW delay line with coupled microstrip lines, but in this case a matched load is connected at the end of the output microstrip line to avoid any reflection. In the '01' codified tag, the matched line is replaced with an open-ended  $\lambda/2$  line in order to produce a total reflection at the end of the line. The tag with the code '10' is identical to the one codified as '00', with the addition of a  $\lambda/2$  line at the centre of the MIW delay line, in order to generate a reflection at half of the total delay time. Finally, the '11' tag has two reflectors. The first one is a  $3\lambda/8$  line to produce a partial reflection and the second one is an open-ended  $\lambda/2$  line to create a total reflection at the end of the line. The length of the first reflector is set to  $3\lambda/8$  because with this line length the pulses of the first and second bit have similar amplitudes, as it will be shown in Fig. 7. This has been concluded after comparing the responses of '11' tags codified with different reflector lengths. A particular aspect of the '11' tag is that multiple reflections occur between the two reflectors. However, the power level of these reflections is much smaller than the pulses corresponding to the identification bits (this will be shown in Fig. 7 where a ripple at 48 ns can be seen). There are mainly two reasons. The first one is that the multiple reflections travel larger distances



through the MIW line. Thus, the propagation losses are much higher. Furthermore, only part of the power is reflected in the first reflector. Thus, each reflection between the two reflectors is attenuated by the reflection coefficient of the first reflector. These facts have also been reported in SAW-based tags [6].

Fig. 6 shows the proposed setup to characterize the chipless tags and obtain their temporal responses. In this scheme, the generator sends a modulated Gaussian pulse at the central frequency of the system ( $f_0 = 2.45$  GHz). After that, the modulated signal is transferred to the chipless tag and its response is obtained through the circulator. The output of the system is the envelope of the signal reflected back by the tag.

The four tags have been simulated by means of *Agilent ADS Momentum* and their temporal responses have been obtained using the proposed setup in a transient simulation of *Agilent ADS*. Fig. 7 shows the temporal response of the four tags. There are pulses at three different times. In all cases, an initial pulse is observed. This is due to certain mismatch at the tag input, so that part of the input signal is reflected back to the envelope detector without being transmitted to the tags. The second group of pulses is obtained after 16 ns approximately, which corresponds to the first identification bit. Finally, the third group of pulses is observed after 32 ns which is the total delay introduced by the MIW delay lines. These pulses correspond to the second bit. Considering -15 dB as the decision threshold, the four different possible codes (00, 01, 10 and 11) are obtained.

The four tags have been fabricated (Fig. 8). These prototypes have been measured by using *Agilent E8364B* network analyzer. Then, their temporal responses have been obtained through the *Agilent ADS* scheme proposed in Fig. 6, and are plotted in Fig. 9. The output signals present a similar shape, although the following considerations must be taken into account. First of all, Fig. 7 and Fig. 9 are normalized to the maximum detected power in each case (at 0 ns). The normalization value is higher in the experimental case, because the reflected power is higher at the input of the fabricated prototypes, as it was shown in Fig. 3. Moreover, the insertion losses in the prototypes are higher than those predicted by the simulator. Hence, the detected power corresponding to the second bit is smaller because the propagation path is twice that of the first-bit path. The consequence of these facts is a higher difference between the levels of the second bit and the normalization value for Fig. 9, as compared to Fig. 7. Nevertheless the groups of pulses corresponding to the first and second bits can be clearly identified at 16 ns and 32 ns, respectively. In this case, the decision threshold has been reduced to -19 dB according to the explanation given before. Considering this threshold, the four tags can be identified properly.

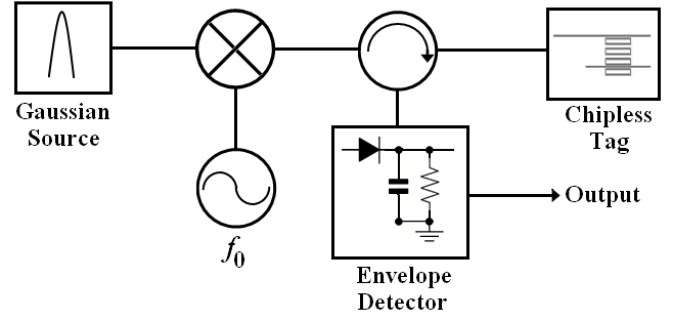


Fig. 6. Proposed setup to obtain the temporal response of the chipless tags.

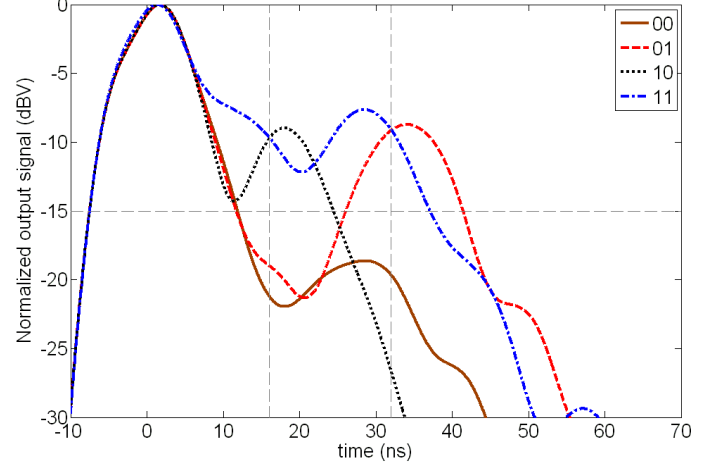


Fig. 7. Simulated temporal response of the four tags.

## V. DISCUSSION

The main limitations of the proposed tags are dispersion and losses of the MIW delay lines. These drawbacks reduce the number of bits that can be stored in the tag, as compared to conventional chip-based tags. This is a general limitation of chipless tags [4]. A possible solution to increase data storage is to use of more complex demodulation schemes, as pointed out in [7]. However, the proposed tags are chipless, and this represents significant cost reduction with respect to conventional tags. If we compare to other chipless solutions (i.e., SAW tags), MIW-based tags are even cheaper since they are fully printed on a dielectric substrate. Hence, low-cost inks and substrates, such as paper, could be used for their implementation, and they could be fabricated as inlays for mass production.

Finally, it would be interesting to estimate the read range of a RFID system based on the proposed tags. This figure of merit can be computed similarly to the case of the SAW chipless tags from the radar equation [6]. The conclusion is that the read range of the system depends on the gain of the reader and tag antennas and the noise figure of the reader. Hence, is not possible to make a correct estimation without actual specifications for the reader. Moreover, a comparison of the read range between chip-based and chipless tags is not straightforward because in conventional chip-based tags the read range is only determined by the characteristics of the tags (the activation power of the chip, the gain of the tag antenna and the matching between the antenna and the chip) and local

regulations (the equivalent isotropic radiated power) [3]. In practical situations, the read ranges of chipless tags are similar or even larger than chip-based tags [4].

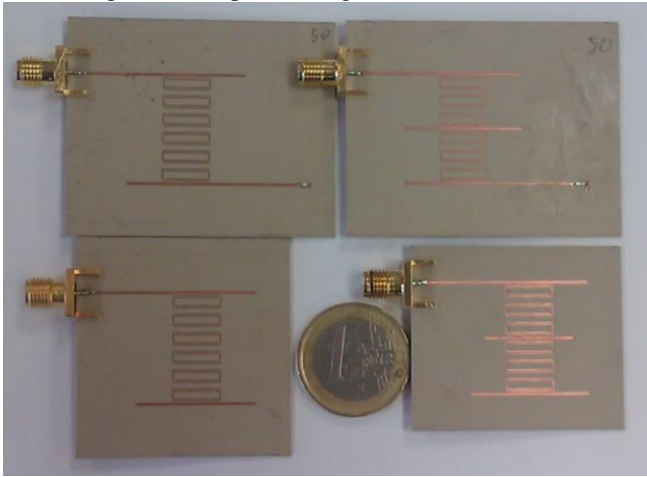


Fig. 8. Photograph of the fabricated set of two-bit chipless tags.

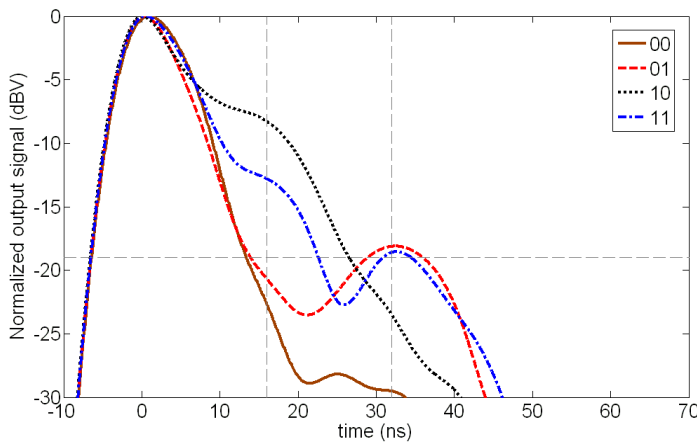


Fig. 9. Temporal response of the four fabricated tags.

## VI. CONCLUSION

A novel fully passive RFID system based on chipless tags has been proposed. These chipless tags are based on periodic MIW delay lines. These lines support the propagation of MIWs, which are slow waves. Thus, large delays can be obtained by using only a small number of cells. This property has been used to codify the identification signature of the proposed tags, achieving small dimensions. The approach is as follows: a band-limited pulse is sent to the MIW delay line based tag, which generates partial reflections of the original pulse at controlled positions within the MIW line. Thanks to the large delay of the MIW line, the replicas of the original pulse are not overlapped in time and can be used to obtain the identification code of the tag.

This work has been focused on the design of the MIW delay lines for the tags. It can be concluded that the MIW lines are useful for the proposed application. However, they are dispersive and exhibit high losses, which can limit the number of bits stored in the line. For this reason, a trade-off between the number of bits, line length, bandwidth and losses must be considered. This can be made by choosing the proper distance

between adjacent SSRRs.

Finally, based on the previous considerations, a complete set of two-bit chipless tag MIW lines has been designed. The simulations and experimental results demonstrate the validity of the proposed approach. These chipless tags are fully printed on a single side of a dielectric substrate and can be easily scaled (e. g. they can be scaled down to operate at higher frequencies). Hence, low-cost substrates could be used. Moreover, the proposed approach is based on time domain demodulation of band-limited signals. Thus, only regulated bands are used, avoiding the interference with other systems. In particular, the 2.45-GHz band is proposed in order to develop a global solution. These characteristics make the proposed tags a good candidate to implement 'RF barcodes'.

## REFERENCES

- [1] K. Finkenzeller *RFID Handbook: Fundamentals and application in contactless smart cards and identification*. John Wiley & Sons, New York, 2003.
- [2] S. Preradovic, N. C. Karmakar, and I. Balbin, "RFID Transponders," *IEEE Microwave Magazine*, vol. 9, no. 5, pp. 90-103, October 2008.
- [3] K.V. Seshagiri Rao, P. V. Nikitin, and S. F. Lam, "Antenna Design for UHF RFID Tags: A Review and Practical Application," *IEEE Transactions on Antennas and Propagation*, vol. 53, no. 12, pp. 3870-3876, Dec. 2005.
- [4] S. Preradovic, and N. C. Karmakar, "Chipless RFID: Bar Code of the Future," *IEEE Microwave Magazine*, vol. 11, no. 7, pp. 87-97, December 2010.
- [5] D. E. N. Davies, M. J. Withers, and R. P. Claydon, "Passive Coded Transponder Using an Acoustic-Surface-Wave Delay Line", *Electronics Letters*, vol. 11, pp. 163-164, 1975.
- [6] L. Reindl, G. Scholl, T. Ostertag, A. Pohl, and R. Weigel, "Wireless Remote Identification and Sensing with SAW Devices", in *Proc. of IEEE 1998 MTT/AP Int. Workshop on Commercial Radio Sensor and Communication Techniques*, pp. 83-96.
- [7] C. S. Hartmann, "A global SAW ID tag with large data capacity," in *Proc. of IEEE Ultrasonics Symposium*, October 2002, vol. 1, pp. 65-69.
- [8] I. Jalaly and D. Robertson, "Capacitively-tuned split microstrip resonators for RFID barcodes," in *Proc. of European Microwave Conference*, October 2005, vol. 2, pp. 4-7.
- [9] J. McVay, A. Hoorfar, and N. Engheta, "Space-filling curve RFID tags," in *Proc. of 2006 IEEE Radio Wireless Symp.*, pp. 199-202.
- [10] S. Mukherjee, "Chipless Radio Frequency Identification by Remote Measurement of Complex Impedance," in *Proc. of the 37th European Microwave Conference*, Munich, Germany, October 2007, pp. 1007-1010.
- [11] S. Preradovic, I. Balbin, N. C. Karmakar, and G. F. Swiegers, "Multiresonator-based chipless RFID system for low-cost item tracking," *IEEE Transactions on Microwave Theory and Techniques*, vol. 57, no. 5, pt. 2, pp. 1411-1419, May 2009.
- [12] S. Preradovic, and N. C. Karmakar, "Design of Chipless RFID Tag for Operation on Flexible Laminates," *IEEE Antennas and Wireless Propagation Letters*, vol. 9, pp. 207-210, 2010.
- [13] H.-S. Jang, W.-G. Lim, K.-S. Oh, S.-M. Moon, and J.-W. Yu, "Design of Low-Cost Chipless System Using Printable Chipless Tag With Electromagnetic Code", *IEEE Microwave and Wireless Components Letters*, vol. 20, no. 11, pp. 640-642, November 2010.
- [14] M. Schüßler, C. Damm, and R. Jakoby, "Periodically LC loaded lines for RFID backscatter applications," in *Proc. of Metamaterials 2007*, Rome, Italy, October 2007, pp. 103-106.
- [15] M. Schüßler, C. Damm, M. Maasch, and R. Jakoby, "Performance evaluation of left-handed delay lines for RFID backscatter applications," in *Proc. of the IEEE MTT-S International Microwave Symposium 2008*, pp. 177-180.
- [16] R. Marqués, F. Martín and M. Sorolla, *Metamaterials with Negative Parameters, theory, design and microwave application*, Hoboken, NJ: John Wiley & Sons, 2008.
- [17] M. J. Freire, R. Marqués, F. Medina, M. A. G. Laso, and F. Martín, "Planar magnetoinductive wave transducers: Theory and applications,"



Applied Physics Letters, vol. 85, no. 19, pp. 4439-4441, November 2004.

- [18] E. Shamonina, V. A. Kalinin, K. H. Ringhofer, and L. Solymar, "Magneto-inductive waveguide", *Electronics Letters*, vol. 38, pp. 371-373, 2002.
- [19] E. Shamonina, V. A. Kalinin, K. H. Ringhofer, and L. Solymar, "Magnetoinductive waves in one, two, and three dimensions", *Journal of Applied Physics*, vol. 92, 6252, 2002.
- [20] M. C. K. Wiltshire, E. Shamonina, I. R. Young, and L. Solymar, "Dispersion characteristics of magneto-inductive waves: comparison between theory and experiment", *Electronics Letters*, vol. 39, pp. 215-217, 2003.
- [21] E. Shamonina and L. Solymar, "Magneto-inductive waves supported by metamaterial elements: components for a one-dimensional waveguide", *Journal of Physics D: Applied Physics*, vol. 37, 362, 2004.
- [22] J.D. Baena, J. Bonache, F. Martín, R. Marqués, F. Falcone, T. Lopetegi, M.A.G. Laso, J. García, I. Gil, M. Flores-Portillo and M. Sorolla, "Equivalent circuit models for split ring resonators and complementary split rings resonators coupled to planar transmission lines", *IEEE Transactions on Microwave Theory and Techniques*, vol. 53, pp. 1451-1461, April 2005.
- [23] K. C. Gupta, R. Garg, I. Bahl, and P. Bhartia, *Microstrip Lines and Slotlines*, 2<sup>nd</sup> ed., Norwood, MA: Artech House, 1996.
- [24] T. S. Rappaport, *Wireless Communications: Principles and Practice*, New Jersey: Prentice Hall, 1996.



**Francisco Javier Herraiz-Martínez** (S'07, M'11) was born in Cuenca, Spain, on May 3, 1983. He received the Engineer and the Ph.D. degrees (both first of his class) in telecommunications from Carlos III University in Madrid, Spain, in 2006 and 2010, respectively.

He spent a year with CIMITEC as a postdoctoral researcher. In October 2012 he joined Carlos III University in Madrid, Spain, where he is currently a

Visiting Lecturer. His research interests include metamaterial applications for antenna and microwave circuits, RFID systems and reconfigurable and active antennas.

Dr. Herraiz-Martínez received the Best Master Thesis Dissertation Award from the COIT/AEIT in 2006. He was recipient of a Spanish Education Ministry official grant for funding his doctoral research activity.



**Ferran Paredes** was born in Badalona (Barcelona), Spain in 1983. He received the Telecommunications Engineering Diploma (specializing in Electronics) and the Telecommunications Engineering degree from the Universitat Autònoma de Barcelona in 2004 and 2006, respectively and the PhD degree in Electronics Engineering from the same university in 2012.

He was Assistant Professor from 2006 to 2008 at the Universitat Autònoma de Barcelona, where he is currently working as a Research Assistant. His research interests include metamaterial concepts, passive microwaves devices, antennas and RFID.

B.S. Degree in Physics from the Universitat Autònoma de Barcelona (UAB) in 1988 and the PhD degree in 1992. From 1994 up to 2006 he has been Associate Professor in Electronics at the Departament d'Enginyeria Electrònica (Universitat Autònoma de Barcelona), and from 2007 he is Full Professor of Electronics. In recent years, he has been involved in different research activities including modelling and simulation of electron devices for high frequency applications, millimeter wave and THz generation systems, and the application of electromagnetic bandgaps to microwave and millimeter wave circuits. He is now very active in the field of metamaterials and their application to the miniaturization and optimization of microwave circuits and antennas. He is the head of the Microwave and Millimeter Wave Engineering Group (GEMMA Group) at UAB, and director of CIMITEC, a research Center on Metamaterials supported by TECNIO (Generalitat de Catalunya). He has organized several international events related to metamaterials, including Workshops at the IEEE International Microwave Symposium (years 2005 and 2007) and European Microwave Conference (2009). He has acted as Guest Editor for three Special Issues on Metamaterials in three International Journals. He has authored and co-authored over 300 technical conference, letter and journal papers and he is co-author of the monograph on Metamaterials entitled Metamaterials with Negative Parameters: Theory, Design and Microwave Applications (John Wiley & Sons Inc.). Ferran Martín has filed several patents on metamaterials and has headed several Development Contracts. Among his distinctions, Ferran Martín has received the 2006 Duran Farell Prize for Technological Research, he holds the Parc de Recerca UAB – Santander Technology Transfer Chair, and he has been the recipient of an ICREA ACADEMIA Award.



**Jordi Bonache** was born in 1976 in Barcelona (Spain). He received the Physics and Electronics Engineering Degrees from the Universitat Autònoma de Barcelona in 1999 and 2001, respectively and the PhD degree in Electronics Engineering from the same university in 2007. In 2000, he joined the "High Energy Physics Institute" of Barcelona (IFAE), where he was involved in the design and implementation of the control and monitoring system of the MAGIC telescope. In 2001, he joined the Department of

Electronics Engineering of the Universitat Autònoma de Barcelona where he is currently Lecturer. From 2006 to 2009 worked as executive manager of CIMITEC. His research interests include active and passive microwave devices and metamaterials.



**Gerard Zamora González** was born in 1984 in Barcelona (Spain). He received the Telecommunications Engineering Diploma, specializing in Electronics from the Universitat Autònoma de Barcelona in 2005. He obtained the Telecommunications Engineering degree in 2008. He is currently working toward his PhD degree at the Universitat Autònoma de Barcelona. His research interests include passive microwave devices based on metamaterial concepts and antenna design for RFID systems.



**Ferran Martín** (M'04-SM'08-F'12) was born in Barakaldo (Vizcaya), Spain in 1965. He received the